Optimization of ply drop locations in variable-stiffness composites

Peeters, D; Abdalla, MM

DOI
10.2514/1.J054369

Publication date
2016

Document Version
Accepted author manuscript

Published in
AIAA Journal: devoted to aerospace research and development

Design guidelines in non-conventional composite laminate optimisation

Daniël Peeters* and Mostafa Abdalla†

Delft University of Technology, 2629 HS Delft, The Netherlands

Non-conventional laminates (NCLs), as defined in this paper, are laminates where ply angles are not restricted to a finite set, for example 0, 45, -45 and 90 degree. Removing this restriction, structural behaviour (e.g., post-impact behaviour) can be significantly improved. NCLs are made of straight or steered fibres leading to constant or variable stiffness composites. In traditional composite design, empirical guidelines are imposed guaranteeing the robustness of the composite. This paper presents a method to take design guidelines into account during NCL optimisation. The 10%-rule is interpreted as a lower bound on the degree of isotropy and formulated as a positive-semi-definite matrix constraint. Other guidelines are interpreted as bounds on ply angle or angle difference, or the number of variables is reduced by fixing variables to user-defined values. Numerical results optimising a plate under bi-axial tension for strength demonstrate the optimiser generates NCLs obeying all guidelines, performing at least as well as conventional composites. For variable stiffness laminates a flat plate under uni-axial compression is optimised for buckling under a stiffness constraint. Applying the 10%-rule, almost half of the improvement over conventional laminates is lost compared to the unconstrained case, demonstrating the importance of including design guidelines during NCL optimisation.

*Ph.D. Student, Faculty of Aerospace Engineering, Aerospace Structures and Computational Mechanics, Kluyverweg 1; D.M.J.Peeters@tudelft.nl; Student member AIAA

†Associate Professor, Faculty of Aerospace Engineering, Aerospace Structures and Computational Mechanics, Kluyverweg 1; M.M.Abdalla@tudelft.nl

Nomenclature

a	inverse of the in-plane stiffness matrix
$\boldsymbol{A}$	in-plane stiffness matrix
c	constant
CL	conventional laminate
CSL	constant stiffness laminate
$\boldsymbol{d}$	damping function
$\boldsymbol{D}$	out-of-plane stiffness matrix
$\mathcal{D}$	feasible region
E	Young's modulus
f	structural response (e.g., buckling, compliance)
$\boldsymbol{g}$	gradient
G	shear modulus
$\boldsymbol{H}$	Hessian
$\boldsymbol{I}$	identity matrix
k	layer number
l	number of layers
L	cholesky factorisation
$\boldsymbol{L}$	Laplacian
m	lower bound on angle difference squared
M	upper bound on angle difference squared
N	total number of nodes
NCL	non-conventional laminate
p	minimum percentage on ply count
s	slack variable
VSL	variable stiffness laminate
x	variable
$\boldsymbol{Z}$	slack matrix
α	minimum of the positive definite problem
δ	change
η	coefficient of mutual influence
γ	degree of isotropy
ν	Poisson's ratio
$\boldsymbol{\epsilon}$	in-plane strain vector
ρ	damping factor
θ	ply angle
λ	Lagrangian multiplier
ϕ	sensitivities w.r.t. the inverse stiffness matrices
ψ	sensitivities w.r.t. the stiffness matrices
subscripts	
0	at the approximation point
b	bending
m	membrane
superscripts	
(1)	level one approximation
(2)	level two approximation

I. Introduction

Composite materials are often used in the aerospace industry because of their high stiffness-to-weight and strength-to-weight ratios. Because the layers have different fibre orientations, the material properties can easily be tailored to the applied load. The percentage of composite material in aircraft has gradually increased since their first use in the 1970s. [1] Some modern aircraft, such as the B-787 and A-350, are in terms of weight made of over 50% composite material. [2, 3]

The different fibre orientations are usually limited to 0°, ±45°, and 90°. This restriction comes from the early days of composite materials when hand lay-up was often used, and these angles could be laid down accurately. Since these fibre orientations have often been used, most available test data is limited to laminates made from these plies, and engineers are more confident using them. Nowadays, sometimes multiples of 15°or 30°are used. [4, 5] Laminates with these restricted sets of possible fibre angles will be referred to as *conventional laminates* (CL) in this paper.

Since conventional laminates are already in use for some decades, design guidelines have been developed over time. Some of these guidelines are motivated by manufacturing concerns, for example having a symmetric laminate. Others are motivated by the need to avoid secondary failure modes, for example the 10% rule. Yet another motivation is based on experience with impact, for example having ±45° surface layers. A lot of experience, that cannot be quantified, is encapsulated in these design guidelines. Adhering to them would make a laminate design more acceptable, and could be a first step towards certification.

During optimisation of conventional laminates, the design guidelines are usually taken into account. [6, 7] Because of the discrete nature of the problem, the most popular optimisation techniques are the direct search and heuristic techniques. [8] The simplest optimisation technique is enumeration, which is only feasible when the number of possibilities is limited. [9] A less computationally expensive method is the use of evolutionary search algorithms; the most popular of which are Genetic Algorithms (GA). [10–12] Other probabilistic search techniques are swarm techniques such as the ant colony optimisation, which was shown to have the same, or better, performance than GAs. [13] These direct search methods employ multiple design rules

within the search algorithm. However, if the number of options increases, even if multiples of 15°are used, the computational cost of evolutionary algorithms is too high.

With the rise of fibre placement machines, the limited set of possible fibre angles disappeared; using these machines, fibres can be laid down accurately in any direction. [14] This increases the ability to tailor the properties of the composite material. Hence, the stiffness-to-weight and strength-to-weight ratios can increase even further. However, the possible fibre angles can now be multiples of 5°, or even smaller, making evolutionary algorithms a computationally very costly option.

Using fibre placement machines, it is also possible to vary the fibre angle within a layer by steering the fibres. [15, 16] This will change the stacking sequence from point to point, and thus also the stiffness. Hence, laminates with steered fibres are referred to as variable stiffness laminates (VSL), while the traditional straight fibre laminates are called constant stiffness laminates (CSL). VSL are described by a different stacking sequence on each node of a finite element model, leading to an optimisation problem with a lot of design variables. [17]

Since every fibre angle can be laid down, the fibre angle can be seen as a continuous variable during optimisation. This means more computationally efficient algorithms such as gradient-based methods can be used. Classical techniques such as the steepest descent or conjugate gradient method have been used for unconstrained optimisation; and sequential quadratic programming and the method of feasible directions for constrained problems. [8] To save computational time response approximation schemes are used. By combining the convex linearisation approximation of Fleury and Braibant [18], the method of conservative convex separable approximations proposed by Svanberg [19], and the method of force approximations proposed by Vanderplaats [20], a good approximation scheme is available to calculate the gradient for a relatively low computational cost. [17]

Another possible approach is optimising the lamination parameters [21]. This has the advantage that at most 12 design variables are present, no matter how many plies the laminate contains. When symmetric laminates are desired, 8 lamination parameters are already sufficient. Optimisation has often been done in terms of lamination parameters. Examples include standard structural responses such as compliance [22], buckling [23, 24], strength [25], and fundamental frequency [26, 27] but the optimisation of aero-elastic properties has been performed as well [28, 29]. Some design guidelines, for example the 10% rule, can be taken into account while optimising the lamination parameters [30]. However, all design guidelines that put limitations on the stacking sequence cannot be interpreted since the stacking sequence is retrieved after the optimisation. The current work only focuses on fibre angle optimisation.

This paper aims at interpreting design guidelines in such a way they can be posed as constraints in a gradient-based optimisation. A lot of design guidelines, such as the 10% rule, are based on counting the number of plies in a certain direction. When the fibre angle is continuous, enforcing these rules on a ply-count basis is impractical. Hence, the guidelines have to be interpreted to be posed as continuous constraints during gradient-based optimisation. Posing the design guidelines as constraints will combine the experience on which these guidelines are based, with the possible advantages of different non-conventional laminate concepts. [31–33] For VSL the constraints are posed at each point.

This paper starts by explaining in detail which non-conventional laminate concepts are considered in section II. Next, an overview of the design guidelines to be implemented is given in section III. How these design guidelines can be posed as continuous constraints is discussed in sections IV to VI. Next, the optimisation formulation, with the design guidelines as constraints, is discussed in section VII. Finally results are presented in section VIII, and the conclusions are given in section IX.

II. Non-conventional laminates

Conventional laminates are defined in this work as laminates made of fibres only containing directions of a limited set. Usually, this set consists of 0°, ±45°, and 90°. [6] Sometimes also multiples of 15°or 30°are used. [4] Laminates with plies in another direction than these are considered to be non-conventional in this work. Using fibre placement machines fibres can be laid down accurately in any direction.

In addition to the angles being possible in any direction, three other types of non-conventional laminates are considered. The first type is a dispersed laminate where a difference in fibre angle between each consecutive ply is implemented. The second type is the advanced placed ply, or APPLY, laminate which mimics the behaviour of woven composites at a fast deposition rate. Both are discussed in more detail in the next two subsections. Finally, the stacking sequence can also be changed from one point to another by steering

the fibres. This leads to variable stiffness laminates (VSL). These are not discussed in more detail in this section.

A. Dispersed laminates

In nature it is observed that parts that have to withstand a lot of impacts, such as claws, have a helical arrangement of mineralised fibre layers. [34] This can be mimicked by having the same change in fibre angle between consecutive layers, as shown in Figure 1. Doing so has been shown to have a positive effect on post-impact behaviour. The difference in fibre angles improves the post impact behaviour, but the in-plane properties are quasi-isotropic this way, reducing the potential weight savings composites may lead to.

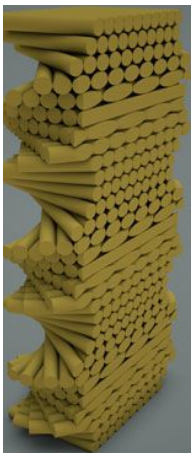

Figure 1. helical dispersing of plies [34]

The good impact resistance is achieved by maintaining a minimal difference in fibre angles between consecutive plies. This reduces the interlaminar shear stress by supporting crack fibre bridging and increasing the number of interfaces (i.e., compared to conventional laminates consecutive plies no longer have the same orientation). Hence, to improve post-impact behaviour, dispersed laminates have a large change in ply angle between consecutive layers to improve impact resistance. [31] This has been shown to improve the post-impact behaviour of composites by Lopes et al. [32, 35] This will be implemented in the optimisation as a lower bound on the change in fibre angle between consecutive plies.

B. APPLY concept

The characteristics of woven plies can be mimicked using the APPLY principle: when laying down 2 layers, first half of the fibres in one direction is laid down, always leaving a gap of exactly one bandwidth, next the fibres in the other direction are laid down, and the gaps are filled in step three and four. This is shown in Figure 2. [33] APPLY combines the advantages of the characteristics of woven plies with the fast and accurate manufacturing using fibre placement machines.

By interweaving the plies using the APPLY principle, delamination is stopped at the edges of the unit cell: the interface between the two plies where the delamination occurred suddenly stops. A unit cell is defined as the area where the stacking sequence is the same: the APPLY principle will lead to different stacking sequences: one some parts it is $[\theta_1/\theta_2]$, in the next unit cell it is $[\theta_2/\theta_1]$. Furthermore, the interwoven plies can be seen as one thick layer, being stiff in two rather than one direction.

Interweaving plies is easiest if the difference between the plies is 90°, as shown in Figure 2. However, as long as a minimal difference between plies is adhered to, they can be interwoven using the APPLY principle. Balanced laminates in this work are defined as follows: for every angle θ, a $-\theta$ is also in the stack. In this work it is assumed balanced pairs of +/- angles are interwoven. To make sure these can be interwoven, an upper and lower bound on fibre angles is implemented: directions too close to 0°or 90°have to be avoided since the unit cell would become very large, hence, the principle of stopping the delamination will not work.

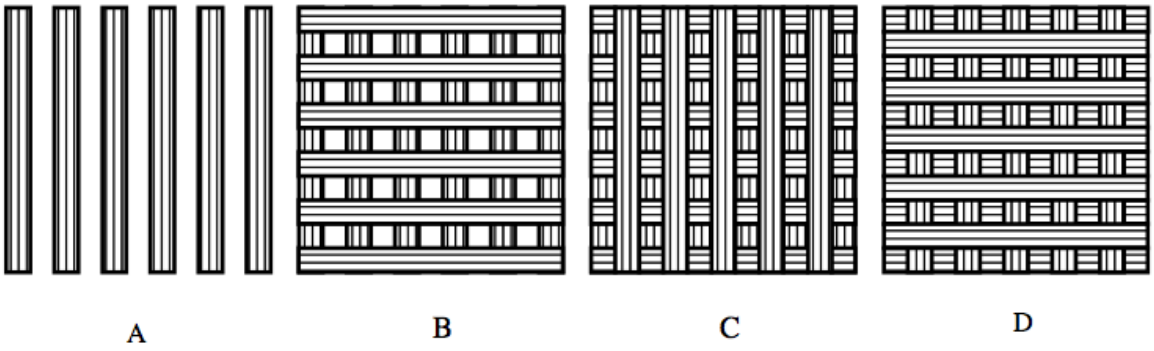

Figure 2. schematic overview of the manufacturing using the APPLY principle [33]

III. Design guidelines

As mentioned in the previous section, dispersed laminates and APPLY have their own limitations, for completeness they are repeated here:

1. For APPLY laminates each layer pair is balanced (i.e., in the form $\pm\theta$). An upper and lower bound on the ply angle is imposed to ensure the size of the unit cell is not too large.
2. For dispersed laminates a lower bound on the difference between adjacent fibre angles is imposed.

Besides these constraints for specific NCL, industry uses constraints on the stacking sequence. The following list is based on the work by Beckwith [36], and a NASA report [37]:

3. The ply contiguity rule, which enjoins the designer to avoid stacking too many plies, usually the limit is set to 4, with the same angle next to each other.
4. Minimise the difference between adjacent fibre angles. If this is not done, the chance of delaminations increases and residual stresses are more likely.
5. The 10 % rule, which states that 10 % of the plies has to be in 0°, 45°, 90°and -45°direction. This makes sure the laminate is not too anisotropic and has at least some resistance against longitudinal (0°), transverse (90°) and shear loading (± 45°). This will also reduce the free-edge stresses and avoid micro-cracking.
6. A laminate should be symmetric about its middle surface. This avoids extension-bending coupling, in other words: the B-matrix is zero.
7. The balance constraint which states that 45°layers should be added in pairs (i.e., with a -45°layer).
8. Put the 45 and -45°layer in contact with each other to minimise interlaminar shear.
9. Add a fabric layer to the inner or outer layer to improve impact damage resistance.
10. Add ±45°layers on outside. This improves the buckling resistance and has a better damage tolerance.
11. Maintain a homogeneous stacking sequence by banding several plies of the same orientation together.
12. keep a reasonable number or primary load-carrying plies away from the outer surfaces. This rule avoids impact damage on the outside to be critical for the primary load-carrying capability.

More guidelines, relating to thermal effects, bonded and bolted joints exist, but since no thermal effects or joints are considered in the current work, these guidelines are not mentioned here.

How the different guidelines are formulated is described in the following sections. First, the bounds on fibre angles, rules 1 - 4, are discussed in section IV. Next, the implementation of the 10 % rule will be

discussed in section V. All remaining guidelines are discussed in section VI. For simplicity, CSL optimisation is assumed in the remainder of the paper: the constraints are local, hence to implement it in VSL optimisation, the constraints have to be posed at each node.

IV. Bounds on angles

Two different bounds on angles exist: the bound on the angle, and the bound on the difference between adjacent angles. For the bounds on the fibre angle, both the lower and upper bound is due to the APPLY principle, rule 1. A lower bound on the change between consecutive plies appears due to the dispersed laminates guideline, rule 2. The maximum number of plies with the same orientation, rule 3, is taken into account by the lower bound on the change in fibre angles without the need to take it explicitly into account: the maximum number of plies with the same orientation is assumed to be one. The final rule implying a bound on the change in fibre angles is rule 4, which states that the change in fibre angles should be minimal: this is implemented as an upper bound on the change in fibre angles.

Since all bounds (lower and upper bound on angle and angle difference) are similar, only the formulation of the upper bound on the difference between adjacent plies will be derived in this section. For the other three constraints, the formulation and implementation will be shown without derivation.

The physical reasoning behind the upper bound on the difference between two adjacent plies are the interlaminar stresses occurring. These arise due to the mismatch in stiffness between the plies with different orientation. According to Herakovich [38], the two most important properties are the Poisson's ratio ν and the coefficient of mutual influence η, defined as

$$\nu_{xy} = \frac{-\epsilon_y}{\epsilon_x} = \frac{a_{12}}{a_{11}} \tag{1}$$

$$\eta_{xy,_x} = \frac{\gamma_{xy}}{\epsilon_y} = \frac{a_{16}}{a_{11}} \tag{2}$$

where $\boldsymbol{a}$ is the inverse of the in-plane stiffness matrix $\boldsymbol{A}$. Using $E_1 = 181\text{GPa}$, $E_2 = 11.3\text{GPa}$, $G_{12} = 7.17\text{GPa}$ and $\nu_{12} = 0.28$ as material data the plots of the Poisson's ratio and the coefficient of mutual influence were made. These are shown in Figure 3.

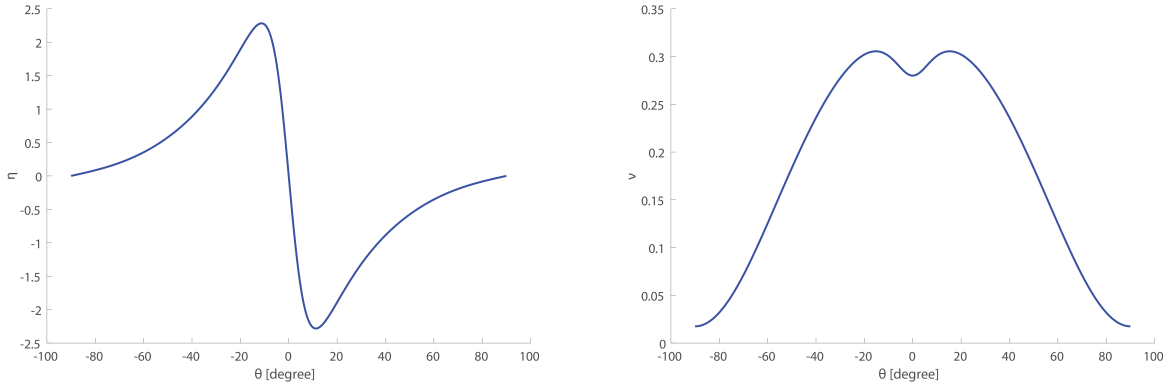

(a) η **(b)** ν

Figure 3. ν **and** η **as a function of the fibre angle**

The difference in ν and η as a function of the difference in angles is the critical factor for interlaminar stresses. The difference in ν and η as a function of the difference between fibre angles, for different average angles (i.e., the average of the two angles, between which the difference is taken, is the same, not the larger or smaller angle), is plotted in Figure 4. The difference in η is clearly very large for small angle differences, hence it will not be taken into account further: it would be too restrictive. Looking at the difference in ν, it is observed that the $\sin(\theta)^2$ matches the shape quite well. When superimposing a $\sin(\theta)^2$ shape on the figure, it can be seen the shape matches well. It captures the periodicity of the difference in Poisson's ratio.

Thus, a constraint is proposed in the form of

$$\sin(\theta_k - \theta_{k+1})^2 \leq \sin(\Delta\theta_{max})^2, \tag{3}$$

where k and k+1 denote the layer of the laminate, and θ_{max} is user-defined, based on the material used.

For the other three bounds, the constraint can be written as:

$$\begin{aligned} \text{lower bound on angle difference} \quad & sin\left(\theta_k - \theta_{k+1}\right)^2 \geq m \quad && k = 1, ..., l-1 \\ \text{upper bound on angle} \quad & sin\left(\theta_k\right)^2 \leq D && k = 1, ..., l \\ \text{lower bound on angle} \quad & sin\left(\theta_k\right)^2 \geq d && k = 1, ..., l, \end{aligned} \tag{4}$$

where $m = \sin(\Delta\theta_{min})^2, d = \sin(\theta_{min})^2$, and $D = \sin(\theta_{max})^2$. The different minimum and maximum angles and angle differences are user-defined. Selected values would reflect the experience with the particular materials system and the type of structural application.

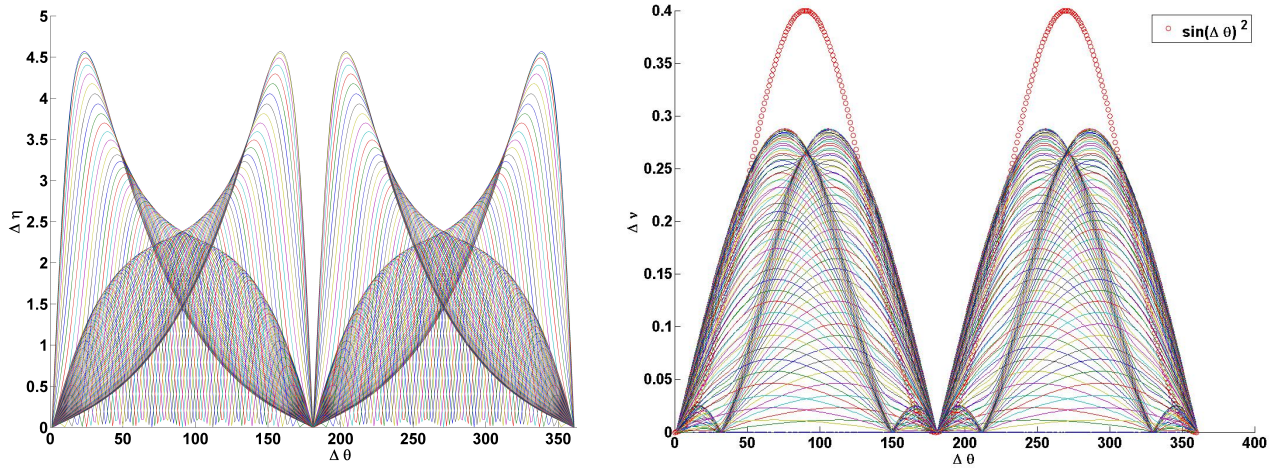

(a) $\Delta\eta$ **(b)** $\Delta\nu$

Figure 4. difference in ν and η as a function of the change in fibre angle

V. 10 % rule

Implementing the 10% rule as stated in section III, is not easy in the context of NCL design. When using a limited set of fibre angles, having a minimum number of layers in each direction can be relatively easily enforced. However, in the current optimisation, the fibre angle is seen as a continuous variable, making it hard to enforce angles of exactly 0°, 90°and ±45°in the optimisation. Furthermore, the 10% rule prescribes at least 40 % of the layers, considerably limiting the design space.

The 10% rule has previously been interpreted by Abdalla et al. as a robustness rule: a minimum stiffness has to be achieved in all directions. [30] This interpretation has been used to replace the ply count-based rule even in the context of CL [4]. The big advantage of this interpretation is that it is continuous. A disadvantage of this stiffness-formulation is the loss of dispersion of the plies, which can be (partly) counter-acted by a lower bound on the change in fibre angle between consecutive plies.

According to Abdalla et al. [30], the 10% rule can be written as a constraint on the minimum eigenvalue of the problem: [30]

$$\boldsymbol{A} : \epsilon = \gamma \bar{\boldsymbol{A}} : \epsilon \tag{5}$$

where ϵ is the in-plane eigen-strain vector; $\bar{\boldsymbol{A}}$ is the quasi-isotropic A-matrix of an arbitrary in-plane stiffness matrix $\boldsymbol{A}$, defined as:

$$\bar{\boldsymbol{A}} = \begin{bmatrix} \bar{A}_{11} & \bar{A}_{12} & 0 \\ \bar{A}_{12} & \bar{A}_{11} & 0 \\ 0 & 0 & \bar{A}_{66} \end{bmatrix} \tag{6}$$

with

$$\bar{A}_{11} = \frac{3A_{11} + 3A_{22} + 2A_{12} + 4A_{66}}{8} \tag{7}$$

$$\bar{A}_{12} = \frac{A_{11} + A_{22} + 6A_{12} - 4A_{66}}{8} \tag{8}$$

$$\bar{A}_{66} = \frac{A_{11} + A_{22} - 2A_{12} + 4A_{66}}{8} \tag{9}$$

The degree of isotropy of the laminate is given by the minimum eigenvalue γ_{min}: the laminate is considered robust if

$$\gamma_{min} \geq \alpha \tag{10}$$

The lower bound on α is dependent on the minimum percentage in ply count p, and on the material used. For carbon material, the lower bound is given by [30]

$$1 - \alpha = \frac{5}{6}(1 - 4p), \tag{11}$$

where the ratio $\frac{5}{6}$ is only valid for carbon material. For the traditional 10% rule $p = 0.1$ and $\alpha = 0.5$.

The eigenvalue constraint can be rewritten as a semi-definite matrix constraint:

$$\left(\boldsymbol{A} - \alpha\bar{\boldsymbol{A}}\right) \succeq 0 \tag{12}$$

Using the Cholesky product, $\bar{\boldsymbol{A}} = \boldsymbol{L} \cdot \boldsymbol{L}^T$, $\boldsymbol{X}$ can be defined as

$$\boldsymbol{X} = \boldsymbol{L}^{-1} \cdot \boldsymbol{A} \cdot \boldsymbol{L}^{-T}, \tag{13}$$

and the constraint on positive semi-definiteness can be written as:

$$\boldsymbol{X} - \alpha \cdot \boldsymbol{I} \geq 0. \tag{14}$$

VI. Other guidelines

The guidelines that are not yet discussed do not require special constraints on the stacking sequence. Some are hard-coded in the optimisation, others are user-defined options. How each guideline can be adhered to is discussed in this section.

The following options define how the *design layers* are related to the actual lay-up:

- the symmetric constraint, rule 6, is hard-coded: every laminate is symmetric, only half the stack, the design layers are optimised, and mirrored to obtain the complete laminate.
- the balance constraint, rule 7, and setting the $\pm 45°$pair next to each other, rule 8, can be implemented by changing the way design layers describe the laminate. If a laminate is to be balanced the design layers $[\boldsymbol{\theta_1/\theta_2}]$ describe the laminate $[\boldsymbol{\theta_1/-\theta_1/\theta_2/-\theta_2}]_S$, meaning a negative angle is added, and if an angle is $45°$, the adjacent angle is $-45°$.
- adding a fabric layer on the outside, rule 9, can be done by defining this layer in the initial guess, and removing this layer from the optimisation. This means that the design layers $[\boldsymbol{\theta_1/\theta_2}]$ describe the laminate $[\text{fabric}/\boldsymbol{\theta_1/-\theta_1/\theta_2/-\theta_2}]_S$, assuming the laminate is to be balanced as well.
- adding the $\pm 45°$layers on the outside, rule 10, can be done in the same way as the fabric layer: by defining the outer layer(s) and removing them from the optimisation. This means that the design layers $[\boldsymbol{\theta_1/\theta_2}]$ describe the laminate $[\boldsymbol{45/-45/\theta_1/-\theta_1/\theta_2/-\theta_2}]_S$, assuming the laminate is to be balanced as well.

The homogeneity rule, rule 11, which states several plies of the same orientation should be bunched together is not implemented. When only four different orientations are possible, from a certain number of plies it is unavoidable to stack plies with the same direction together. When this happens, the question whether or not to group them arises. However, the orientation is continuous in this work, so it can be avoided

to have the same orientation next to each other, hence the need for this rule does not arise. Furthermore, this rule directly contradicts the idea of dispersed laminates, rule 2.

Finally, rule 12, which states that a reasonable number of primary load-carrying plies should be kept away from the outer surfaces is not implemented. This has two reasons. One, the outer surface can already be defined if wanted: depending on the load case, a $\pm 45°$ply is usually not considered to be a primary load-carrying ply, hence defining it on the outside can be done. Two, this rule relies on engineering judgement: it cannot be formulated as a constraint. The idea behind the rule, which is improving the impact-resistance, is implemented using the dispersed and/or APPLY laminates.

VII. Optimisation procedure

In structural optimisation, the minimisation of an objective response (e.g., weight or compliance) subject to performance constraints (e.g., on stresses or displacements) is studied. More generally, the worst case response, for example in the case of multiple load cases, is optimised. Additional constraints not related to structural responses may also be imposed to guarantee certain properties of the design such as manufacturability. The following general problem formulation is considered:

$$\begin{array}{ll} \min\limits_{\boldsymbol{x}} & \max\limits_{n}(f_1, f_2, ..., f_n) \\ s.t. & f_{n+1}, ..., f_m \leq 0 \\ & \boldsymbol{x} \in \mathcal{D}. \end{array} \tag{15}$$

The functions f_i depend on the design variables; f_1 to f_n denote structural responses that are optimised and f_{n+1} to f_m denote structural responses that are constrained. In addition to these constraints, the guideline constraints are added. For VSL, additional constraints guaranteeing manufacturability are posed. These manufacturing constraints are outside the scope of this paper, the interested reader is referred to earlier work by the authors [17]. The linear finite element analysis is performed using our own Matlab implementation. The sensitivity analysis and construction of the approximations are not discussed in this paper; the interested reader is referred to earlier work [17, 25, 39, 40]. The feasible region is denoted by $\mathcal{D}$. This problem is solved using successive approximations: starting from a certain fibre angle distribution, the approximations are constructed based on this fibre angle distribution, the approximations are optimised and the approximations are updated based on the new fibre angle distribution. The optimisation of the approximate sub-problem is performed using a predictor-corrector interior-point method. This is repeated until convergence is reached. Convergence is defined in this work by the change in objective function: if this is smaller than a certain threshold, usually 10^{-3} is used, the solution is assumed to be converged.

When implementing the design guidelines, two different types of constraints appear: one, functional constraints, based on the bounds on angle and angle difference, eqs. (3)-(4), two, the positive semi-definite matrix constraint, based on the ply-count percentage rule, eq. (14). To keep the derivation as simple as possible and focus on the design guideline constraints, a single-response optimisation without constraints on structural performance is considered:

$$\begin{array}{lll} \min\limits_{\boldsymbol{x}} & f & \\ s.t. & \boldsymbol{X} - \alpha \cdot \boldsymbol{I} \geq 0 & \\ & g\left(\theta_k, \theta_{k+1}\right) & k = 1, ..., l-1 \\ & h\left(\theta_k\right) & k = 1, ..., l \end{array} \tag{16}$$

where l denotes the total number of layers. The functions g and h (which denote the different constraints on angle difference and angle respectively) are linearised. The linearised versions are referred to as $\hat{g}$ and $\hat{h}$. $\boldsymbol{X}$ can be linearised as well. It is approximated as:

$$\boldsymbol{X} = \boldsymbol{X}_0 + \sum_{i=1}^{L} \boldsymbol{X}_i x_i, \tag{17}$$

where, referring to eq. (13), $\boldsymbol{X}_i$ is defined as

$$\boldsymbol{X}_i = \boldsymbol{L}^{-1} \cdot \frac{\partial \boldsymbol{A}}{\partial x_i} \cdot \boldsymbol{L}^{-T}. \tag{18}$$

A slack variable s and a damping function d, to guarantee global convergence, which is multiplied with a damping factor ρ are added for both functional constraints. For more information about the damping function, the reader is referred to earlier work by the authors [17]. For the positive semi-definite matrix, a slack matrix $\boldsymbol{Z}$ is added, and the damping function d is multiplied with an identity matrix of the appropriate size. The optimisation problem now takes the form:

$$\begin{aligned}
\min_{\boldsymbol{x}} \quad & f + \rho_1 d_1(x) \\
s.t. \quad & \boldsymbol{X}_0 + \textstyle\sum_{i=1}^{L} \boldsymbol{X}_i x_i - \alpha \cdot \boldsymbol{I} - \rho_2 \cdot d_2(x) \cdot \boldsymbol{I} - \boldsymbol{Z} = \boldsymbol{0} \\
& \hat{g}\left(\theta_k, \theta_{k+1}\right) + \rho_3 \cdot d_{(3k)}(x) + s_g = 0 \qquad k = 1, ..., l-1 \\
& \hat{h}\left(\theta_k, \theta_{k+1}\right) + \rho_4 \cdot d_{(4k)}(x) + s_h = 0 \qquad k = 1, ..., l-1 \\
& \boldsymbol{Z} \geq 0 \\
& s_g \geq 0 \\
& s_h \geq 0
\end{aligned} \tag{19}$$

The damping functions are defined as:

$$d_2 = \Delta\theta \left(\frac{1}{n_l^2} \begin{bmatrix} 1 & -1 & & & & \\ -1 & 2 & -1 & & & \\ & \ddots & \ddots & & & \\ & & -1 & 2 & -1 & \\ & & & -1 & 1 & \end{bmatrix} + \alpha \begin{pmatrix} 1 & \dots & 1 \\ \vdots & \ddots & \vdots \\ 1 & \cdots & 1 \end{pmatrix} \right) \cdot \Delta\theta \tag{20}$$

$$d_{(3k)}(x) = \frac{\left(\Delta\theta_k - \Delta\theta_{k+1}\right)^2}{2} \tag{21}$$

$$d_{(4k)}(x) = \frac{\left(\Delta\theta_k\right)^2}{2}, \tag{22}$$

where n_l denotes the number of layers. Next, the Lagrangian is found

$$\begin{aligned}
\mathcal{L} = {} & f(x) + \rho_1 d_1(x) - \boldsymbol{Y} : \left(\boldsymbol{X}_0 + \sum_{i=1}^{L} \boldsymbol{X}_i x_i - \alpha \cdot \boldsymbol{I} - \rho_2 d_2(x) \cdot \boldsymbol{I} - \boldsymbol{Z} \right) - \mu ln\left(det(\boldsymbol{Z})\right) + \\
& \sum_k \lambda_k \cdot \left(\hat{g} + \rho_3 d_{(3k)}(x) + s_{g_k} \right) + \mu \cdot ln(s_{g_k}) + \sum_k \gamma_k \cdot \left(\hat{h} + \rho_4 d_{(4k)}(x) + s_{h_k} \right) + \mu \cdot ln(s_{h_k}).
\end{aligned} \tag{23}$$

The solution procedure is explained in Appendix A.

VIII. Results

To assess the influence of the different constraints, two examples will be used: a strength optimisation for a CSL, and a buckling optimisation for a VSL. In each case, the starting point has to be feasible, since the interior point method should conserve feasibility, but it requires a feasible starting point. It will be checked that the final solution is still feasible. For the CSL the influence on the ply-count percentage rule is investigated, and the influence of the bounds on the angles and angle difference. For the VSL only the influence of the ply-count percentage rule is investigated.

A. Constant Stiffness Laminates

A strength optimisation is performed for CSLs. The model is a square panel with sides of 500 mm, simply supported all around, and with the edges constrained to remain straight. The plate is loaded under bi-axial tension N_x and N_y. A graphical representation can be seen in Figure 5. The material used has the following properties: $E_1 = 154$GPa, $E_2 = 10.8$GPa, $G_{12} = 4.02$GPa, $\nu_{12} = 0.317$, $t_{ply} = 0.6$mm. The laminate consists of 36 layers, and is balanced and symmetric, meaning 9 design layers are optimised. Failure is defined using the *conservative* omni-strain envelope [25, 40, 41]. The factor of safety, which is the inverse of the failure

index, is normalised with respect to a quasi-isotropic laminate, defined as all lamination parameters equal to zero in this work. Lamination parameters provide a way to describe the stiffness properties of a laminate without defining a lay-up, more information can be found in for example Tsai and Hahn [21]. Since strength, is an in-plane property, the behaviour is the same as a laminate with an equal amount of 0°, 45°, −45°, and 90° plies, when defined using the omni-strain envelope. When using more traditional criteria such as Tsai-Wu, the strength of two quasi-isotropic laminates with different layups may differ.

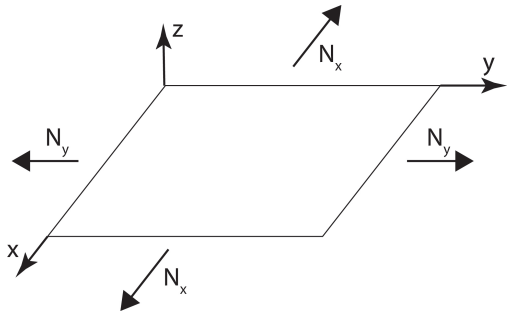

Figure 5. Sketch of the plate loaded in tension.

Influence of the ply-count percentage rule

The influence of the ply-count percentage constraint, or 10% rule, is investigated: different values for the ply-count percentage are checked, without any bound on the angles or angle difference. Only one ratio of the loads is checked: $N_y/N_x = 1/6$. First, the optimisation is performed without the constraint. The optimal laminate then has a ply-count percentage of 3.67%, and a factor of safety of 2.72. Next, the optimisation is repeated for values of the ply-count percentage from 4 to 16%. The normalised factor of safety for both conventional and non-conventional laminates is shown in Figure 6. The conventional design is found by enumeration: the performance of all conventional designs and selecting the best one. Since the factor of safety is optimised, only the in-plane stiffness matrix has an influence on the performance of the structure, meaning only the number of layers with a certain orientation is important, not their location in the stack. This means enumeration can be done by checking a limited number of options, hence for the conventional design the global optimum is found.

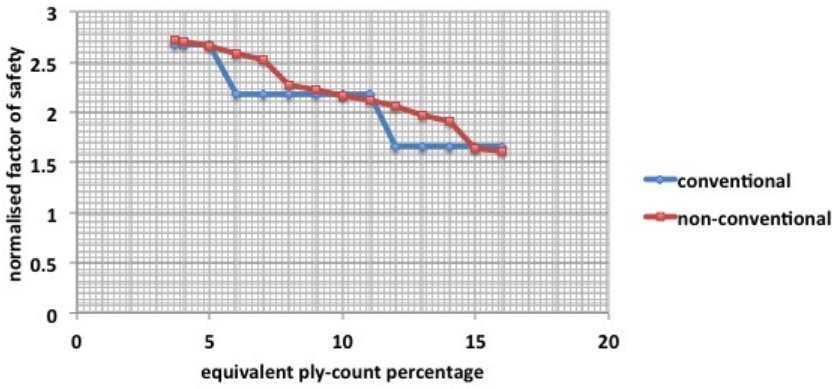

Figure 6. Factor of safety for different values of the ply-count percentage, both for conventional(blue) and non-conventional (red) laminates.

Looking at the results it is noted that the general trend is as expected: the larger the bound on ply-count percentage, the lower the factor of safety is. The graph in Figure 6 is monotonically decreasing, as it should be. During the numerical experiments it was observed that sometimes a better performance was

found with a higher bound on ply-count percentage, depending on the initial guess. Since the optimisation is not computationally expensive, and it is well-known that a gradient-based optimiser can get stuck in a local optimum, multiple initial guesses were used, and only the best is shown. Another interesting point are the drops at 8 and 15%. These are most likely caused by the optimiser getting pushed to a different local optimum since the direction for the optima found for lower values of the ply-count percentage constraint is no longer feasible. This shows that local optima can work both ways: one can get lucky and find a better local optimum with a higher robustness constraint, or the performance significantly decreases.

The conventional design stays constant for a certain range of ply-count percentages: since the laminate has to be balanced and symmetric, and consists of 36 layers in total, most of the time the ply-count percentage is higher than it strictly has to be. At places where the conventional design is very conservative with respect to the ply-count percentage, the non-conventional one is clearly outperforming the conventional design. This demonstrates a secondary advantage using non-conventional laminates: the design is not more conservative than it needs to be, leading to a better performance. For the cases where the constraint on the non-conventional design and the actual percentage of the conventional design are close to each other, the performance is very close as well. At some places the conventional design is even performing slightly better than the non-conventional one. This is due to the optimiser getting stuck in a local optimum, while for the conventional design the global optimum is found.

Influence of other design guidelines

All constraints implemented are active: the 'traditional' 10% rule is used as ply-count percentage, a lower bound on the angle of 5°is used, an upper bound on the angle of 85°, a lower bound on the angle difference of 10°and an upper bound on the angle difference of 45°. The same problem is optimised, for a range of ratios N_y/N_x. By increasing the ratio from 0 to 1, the optimal design will get closer and closer to the quasi-isotropic design. With a ratio of 1 the optimal design should be a quasi-isotropic laminate.

As was shown in the previous part, the optimisation is prone to getting stuck in a local optimum. This is an inherent disadvantage of using a gradient-based optimisation. The advantage is that the optimisation is quite quick, thus multiple starting points can be checked. The results for different ratios and different starting points are shown in Table 1. Start 1 is $[\pm 10/\pm 40/\pm 70/\pm 45/\pm 30/\pm 50/\pm 75/\pm 40/\pm 15]_s$, start 2 is $[\pm 6/\pm 17/\pm 28/\pm 39/\pm 50/\pm 61/\pm 72/\pm 63/\pm 50]_s$, and start 3 is $[\pm 30/\pm 60/\pm 30/\pm 60/\pm 30/\pm 60/\pm 30/\pm 60/\pm 30]_s$.

The results show the normalised factor of safety. Normalisation is always done with respect to the factor of safety for the specific loading condition. All constraints are satisfied for all optimised results: each optimised design is feasible.

Table 1. Factor of safety normalised with respect to the quasi-isotropic factor of safety for different ratios of N_y/N_x

ratio	start 1	start 2	start 3
0	1.522	1.156	1.266
0.25	1.870	1.815	1.431
0.5	1.543	1.638	1.635
0.75	1.222	0.999	1.220
1	0.995	0.995	0.999

Observing the results in Table 1 it is noticed that the factor of safety for the different starting points can differ significantly, showing again that the optimisation is prone to getting stuck in a local optimum. However, except for a ratio of 0, meaning uni-axial loading in x-direction, the highest two values are close together. From a ratio of 0.25 onward, the normalised factor of safety is always decreasing, indicating that the laminate is getting closer to the behaviour of a quasi-isotropic laminate. This is expected since the closer the ratio of N_y/N_x gets to one, the closer the ideal stiffness E_y/E_x gets to one, and thus the closer the laminate gets to quasi-isotropic behaviour.

For a ratio of 1, the theoretical optimum is a quasi-isotropic laminate, and this is almost what was found. At least, the performance of the laminate is almost identical to a quasi-isotropic one: the lay-up, however, for the three optima is very different. From start 1, the optimum found is $[\pm 13/\pm 34/\pm 69/\pm 48/\pm 31/\pm$

$58/\pm 79/\pm 51/\pm 21]_s$, from start 2 $[\pm 8/\pm 20/\pm 30/\pm 40/\pm 50/\pm 66/\pm 83/\pm 65/\pm 42]_s$, and from start 3 $[\pm 28/\pm 59/\pm 32/\pm 60/\pm 31/\pm 63/\pm 34/\pm 67/\pm 33]_s$. This proves that different lay-ups may lead to (almost) the same stiffness properties, and hence the same factor of safety.

B. Influence of the ply-count percentage rule on VSL

To assess the influence the ply-count percentage has on the performance of a VSL, a different optimisation problem is chosen since a CSL is optimal for the bi-axial loading case of the previous section. The problem for VSL is defined as a buckling optimisation of a flat plate of 400 by 600 mm, under uni-axial compression on the short edge, with a stiffness constraint: the stiffness has to be at least the stiffness of a quasi-isotropic laminate. A graphical representation can be seen in Figure 7. The plate is meshed using 1200 triangular elements and 651 nodes. By taking symmetry into account, the stacking sequence has to be optimised at 176 nodes. At each node the ply-count percentage has to be satisfied. A minimum steering radius of 333 mm is imposed to ensure the laminate is manufacturable. This is imposed at each design layer and each of the 300 elements in the symmetric model. The same material is used as in the previous example, and the laminate consists of 36 layers, which due to balance and symmetry is equivalent to 9 design layers. Since the stacking sequence at each node is to be found, over 1500 design variables are present in this problem.

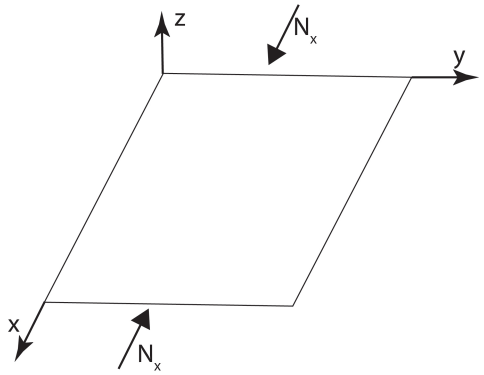

Figure 7. Sketch of the plate loaded in compression.

An exhaustive search for the best conventional lay-up is not possible: the position of the layers is important for a buckling optimisation, hence the number of possible stacking sequences is too large to be enumerated. Rather, a suitably efficient reference design is constructed: the number of $\pm 45°$plies is maximised, and the minimum number of 0 degree layers is determined based on the stiffness constraint, for which the place in the stack is not important. Next, the layers found are shuffled to find the reference design. This lay-up is found to be $[\pm 45/0/\pm 45/90/\pm 45/0/\pm 45/0/\pm 45/90/0_2/\pm 45/0_2]_s$.

As in the CSL case, the optimisation is first performed without a constraint on the ply-count percentage. The starting point was chosen to be $[\pm 40/\pm 70/\pm 40/\pm 10/\pm 70/\pm 70/\pm 10/\pm 40/\pm 10]$. The ply-count percentage of the optimal design was found to be 0.57%. This low equivalent ply-count percentage is mainly caused by the stacking sequence near the centre of the plate which consists almost exclusively of $\pm 45°$layers. On the panel sides the ply count percentage is higher due to the stiffness constraint. Next, the optimisation is performed varying the ply-count percentage constraint from 1 until 12%. The results, normalised with respect to the reference conventional lay-up, are shown in Figure 8.

Looking at the results, it is noticed that steering without any constraint on the ply-count percentage, 53.5% improvement in buckling load can be obtained, while when applying the 'traditional' 10% rule, only a 28.2% improvement can be obtained. Hence, almost half of the improvement over conventional laminates is lost due to the ply-count percentage rule. This is due to the restricted possibility for stiffness changes over the panel, which causes a reduction in the load redistribution, and hence a reduction in the buckling load with respect to the unconstrained laminate. However, an improvement of more than 28% is still significant. Furthermore, by adhering to the 10% rule, these laminates are more likely to be used in practical structures. Hence, by sacrificing some performance (16.5% compared to the optimal steered panel), the feasibility of the design is increased. The exact ply-count percentage that has to be used is case-dependent. For example,

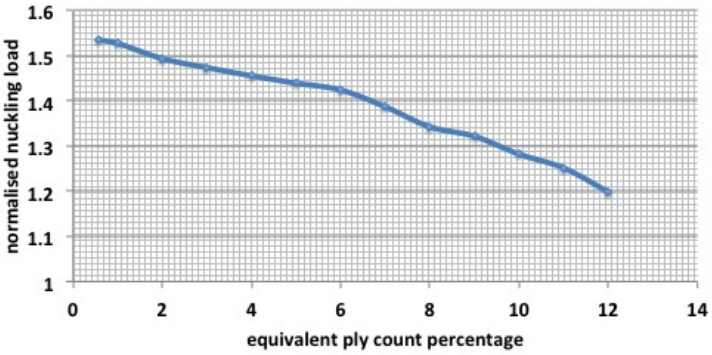

Figure 8. Optimal factor of safety for different ply-count percentages, normalised with respect to the reference conventional laminate.

at a minimum ply-count percentage of 5%, the performance is 43.9% higher than the reference conventional laminate.

IX. Conclusion

In this paper a method to pose design guidelines as constraints in a gradient-based optimisation is described. Different rules concerning bounds on angles and angle difference were implemented. The ply-count percentage, the 'traditional' 10% rule, was interpreted as a minimum degree of isotropy. This was then implemented as a positive semi-definite matrix constraint. Convex approximations of the structural responses are made in terms of the fibre angles. The method of successive approximations was used in combination with a predictor-corrector interior-point method to perform the optimisation.

A square plate simply supported all around under bi-axial tension N_x, N_y is optimised to improve the factor of safety. The laminate is a constant-stiffness laminate. Numerical results indicate that the optimisation method succeeds in satisfying all guideline constraints. It was observed the optimisation got stuck in a local optimum, which is expected since the problem is highly non-convex. Hence, multiple initial guesses were used. First, the influence of the ply-count percentage was checked for a fixed value of the ratio between N_x and N_y. Results were as expected: the higher the lower bound on degree of isotropy, the lower the factor of safety. Second, multiple ratios of N_y/N_x were investigated, and the lower bound on degree of isotropy, and bounds on the ply angle and angle difference were posed. This optimisation confirmed that the constraints were satisfied in each case, but the results were dependent of the initial guess. Although the results were dependent on the initial guess, comparable performance for different initial guesses was obtained.

Numerical results for variable stiffness laminates show that by implementing the ply-count percentage rule a rather large part of the improvement with respect to conventional laminates is lost. When the 10% rule was implemented about half of the improvement was lost, which can be explained by the smaller change in stiffness over the panel, and thus also less load redistribution. On the other hand: by implementing the ply-count percentage rule, the feasibility and applicability of the laminate increases significantly.

The results showed the importance of implementing the design guidelines in the optimisation formulation. Multiple laminates having (almost) the same performance, but different lay-up were identified, all obeying the design guidelines. This shows one of the reasons for the multiple local optima: lay-ups that look completely different at first sight may have similar structural behaviour. While from an optimisation point-of-view these multiple optima are hard to handle, they may have benefits as well: other considerations can determine which of the lay-ups is best suited at a certain location. Hence, these multiple optima give the user a set of possible lay-ups, which can be judged from a different perspective, without compromising structural performance.

X. Acknowledgements

This work is supported by the CANAL (CreAting Non-conventionAl Laminates) Project, part of the European Union Seventh Framework Program.

A. Solution procedure of the optimisation problem

Starting from the Lagrangian, eq. (23), the matrices of the positive semi-definite constraint are rewritten. Instead of the 2-dimensional arrays $\boldsymbol{X}_i$, one can also define a 3-dimensional array $\boldsymbol{\mathcal{X}}$, such that $\boldsymbol{\mathcal{X}}_{abi} = \boldsymbol{X}_i$. Defining two operators:

$$\boldsymbol{\mathcal{X}}^T \cdot \boldsymbol{Y} = \sum_{i=1}^{L} \boldsymbol{\mathcal{X}}_{abi} \cdot \boldsymbol{Y}_{ab} \tag{24}$$

$$\boldsymbol{\mathcal{X}} \cdot \boldsymbol{x} = \sum_{i=1}^{L} \boldsymbol{\mathcal{X}}_{abi} \cdot \boldsymbol{x}_i. \tag{25}$$

The optimality conditions are found to be

$$\begin{aligned}
-r_{x_j} &= \boldsymbol{g} + \rho_1 \cdot \boldsymbol{g}^{(1)} - \boldsymbol{\mathcal{X}}^T \cdot \boldsymbol{Y} + \rho_2 \left(\boldsymbol{Y} : \boldsymbol{I}\right) \boldsymbol{g}^{(2)} + \\
&\quad \sum_k \lambda_k \cdot \left(\frac{\partial \hat{g}}{\partial x_j} + \rho_3 \cdot \frac{\partial d_{3k}}{\partial x_j} \right) + \sum_k \gamma_k \cdot \left(\frac{\partial \hat{h}}{\partial x_j} + \rho_4 \cdot \frac{\partial d_{4k}}{\partial x_j} \right) \\
-r_{\lambda_k} &= \hat{g} + \rho_3 \cdot d_{(3k)}(x) + s_{g_k} \\
-r_{\gamma_k} &= \hat{h} + \rho_4 \cdot d_{(4k)}(x) + s_{h_k} \\
-r_{s_{g_k}} &= \lambda_k \cdot s_{g_k} - \mu \\
-r_{s_{h_k}} &= \gamma_k \cdot s_{h_k} - \mu \\
-r_{\boldsymbol{Y}} &= -\boldsymbol{X}_0 - \boldsymbol{\mathcal{X}}^T \cdot \boldsymbol{x} + \alpha \cdot \boldsymbol{I} + \rho_2 d_2(x) \cdot \boldsymbol{I} + \boldsymbol{Z} \\
-r_{\boldsymbol{Z}} &= \boldsymbol{Z} \cdot \boldsymbol{Y} - \mu \cdot \boldsymbol{I},
\end{aligned} \tag{26}$$

where the criteria of the slack variables have been multiplied with the slacks to avoid numerical problems. [42] Linearising these equations leads to

$$\begin{aligned}
r_{x_j} &= \boldsymbol{H} \cdot \boldsymbol{dx} + \rho_1 \boldsymbol{H^{(1)}} \cdot \boldsymbol{dx} + \rho_2 \left(\boldsymbol{Y} : \boldsymbol{I}\right) \cdot \boldsymbol{H^{(2)}} \cdot \boldsymbol{dx} - \boldsymbol{\mathcal{X}}^T \cdot \boldsymbol{dY} + \rho_2 \left(\boldsymbol{dY} : \boldsymbol{I}\right) \cdot \boldsymbol{g}^{(2)} + \\
&\quad \left(\frac{\partial \hat{g}}{\partial x_j} + \rho_3 \cdot \frac{\partial d_{3k}}{\partial x_j} \right) d\lambda_k + \left(\frac{\partial \hat{h}}{\partial x_j} + \rho_4 \cdot \frac{\partial d_{4k}}{\partial x_j} \right) d\gamma_k \\
r_{\gamma_k} &= \sum_j \frac{\partial \hat{h}}{\partial \theta_j} dx_j + \rho_4 \sum_j \frac{\partial d_{4j}}{\partial \theta_j} dx_j + ds_{h_k} \\
r_{\lambda_k} &= \sum_j \frac{\partial \hat{g}}{\partial \theta_j} dx_j + \rho_3 \sum_j \frac{\partial d_{3j}}{\partial \theta_j} dx_j + ds_{g_k} \\
r_{s_g} &= d\lambda_k \cdot s_{g_k} + \lambda \cdot ds_{g_k} \\
r_{s_h} &= d\gamma_k \cdot s_{h_k} + \lambda \cdot ds_{h_k} \\
r_{\boldsymbol{Y}} &= -\boldsymbol{\mathcal{X}} \cdot \boldsymbol{dx} + \rho_2 \left(\boldsymbol{g}^{(2)T} \cdot \boldsymbol{dx} \right) \cdot \boldsymbol{I} + \boldsymbol{dZ} \\
r_{\boldsymbol{Z}} &= \boldsymbol{dZ} \cdot \boldsymbol{Y} + \boldsymbol{Z} \cdot \boldsymbol{dY}.
\end{aligned} \tag{27}$$

Defining $\boldsymbol{\lambda}$, $\boldsymbol{\gamma}$, $\boldsymbol{S_g}$ and $\boldsymbol{S_h}$ as the diagonal matrices containing λ_k, γ_k, s_{g_k} and s_{h_k} on their diagonal, the linearisation can be rewritten as

$$\begin{aligned} r_x &= \boldsymbol{H_i} \cdot \boldsymbol{dx} - \boldsymbol{\mathcal{X}}^T \cdot \boldsymbol{dY} + \rho_2 \left(\boldsymbol{dY} : \boldsymbol{I}\right) \cdot \boldsymbol{g}^{(2)} + \hat{\boldsymbol{G}}^T \boldsymbol{d\lambda} + \hat{\boldsymbol{H}}^T \boldsymbol{d\gamma} \\ r_\lambda &= \hat{\boldsymbol{G}} \cdot \boldsymbol{dx} + \boldsymbol{dS_g} \\ r_\gamma &= \hat{\boldsymbol{H}} \cdot \boldsymbol{dx} + \boldsymbol{dS_h} \\ r_{S_g} &= \boldsymbol{d\lambda} \cdot \boldsymbol{S_g} + \boldsymbol{\lambda} \cdot \boldsymbol{dS_g} \\ r_{S_h} &= \boldsymbol{d\gamma} \cdot \boldsymbol{S_h} + \boldsymbol{\gamma} \cdot \boldsymbol{dS_h} \end{aligned} \tag{28}$$

where the rows k of $\hat{\boldsymbol{G}}$ and $\hat{\boldsymbol{H}}$ are constructed according to

$$\hat{\boldsymbol{G}}_k = \frac{\partial \hat{g}_k}{\partial x_j} + \rho_3 \cdot \frac{\partial d_{3k}}{\partial x_j} \tag{29}$$

$$\hat{\boldsymbol{H}}_k = \frac{\partial \hat{h}_k}{\partial x_j} + \rho_4 \cdot \frac{\partial d_{4k}}{\partial x_j} \tag{30}$$

$\boldsymbol{dS_g}$, $\boldsymbol{dS_h}$, $\boldsymbol{d\lambda}$, $\boldsymbol{d\gamma}$, $\boldsymbol{dZ}$, and $\boldsymbol{dY}$ can be found to be

$$\begin{aligned} \boldsymbol{d\lambda} &= \boldsymbol{S_g}^{-1} \cdot \left(\boldsymbol{r_{s_g}} - \boldsymbol{\lambda} \boldsymbol{dS_g}\right) \\ \boldsymbol{d\gamma} &= \boldsymbol{S_h}^{-1} \cdot \left(\boldsymbol{r_{s_h}} - \boldsymbol{\gamma} \boldsymbol{dS_h}\right) \\ \boldsymbol{dS_g} &= \boldsymbol{r_\lambda} - \hat{\boldsymbol{G}} \boldsymbol{dx} \\ \boldsymbol{dS_h} &= \boldsymbol{r_\gamma} - \hat{\boldsymbol{H}} \boldsymbol{dx} \\ \boldsymbol{dZ} &= r_{\boldsymbol{Y}} + \boldsymbol{\mathcal{X}} \cdot \boldsymbol{dx} - \rho_2 \left(\boldsymbol{g}^{(2)T} \cdot \boldsymbol{dx}\right) \cdot \boldsymbol{I} \\ \boldsymbol{dY} &= \boldsymbol{Z}^{-1} \cdot r_{\boldsymbol{z}} - \boldsymbol{Z}^{-1} \cdot \boldsymbol{dZ} \cdot \boldsymbol{Y}. \end{aligned} \tag{31}$$

Filling this into the equation for r_x leads to

$$\begin{aligned} r_x = \; & \boldsymbol{H_i} \cdot \boldsymbol{dx} + \rho_2 \left(\left(\boldsymbol{Z}^{-1} \boldsymbol{r_z} - \boldsymbol{Z}^{-1} \left(\boldsymbol{r_y} + (\boldsymbol{\mathcal{X}} \cdot \boldsymbol{dx}) - \rho_2 \left(\boldsymbol{g}^{(2)T} \boldsymbol{dx} \right) \boldsymbol{I} \right) \boldsymbol{Y} \right) : \boldsymbol{I} \right) \boldsymbol{g}^{(2)} - \\ & \boldsymbol{\mathcal{X}}^T \cdot \left(\boldsymbol{Z}^{-1} \boldsymbol{r_z} - \boldsymbol{Z}^{-1} \left(\boldsymbol{r_y} + \boldsymbol{\mathcal{X}} \cdot \boldsymbol{dx} - \rho_2 \left(\boldsymbol{g}^{(2)T} \boldsymbol{dx} \right) \boldsymbol{I} \right) \boldsymbol{Y} \right) + \\ & \hat{\boldsymbol{G}}^T \cdot \boldsymbol{S_g}^{-1} \cdot \left(\boldsymbol{r_{s_g}} - \boldsymbol{\lambda} \left(\boldsymbol{r_\lambda} - \hat{\boldsymbol{G}} \boldsymbol{dx} \right) \right) + \hat{\boldsymbol{H}}^T \cdot \boldsymbol{S_h}^{-1} \cdot \left(\boldsymbol{r_{s_h}} - \boldsymbol{\gamma} \left(\boldsymbol{r_\gamma} - \hat{\boldsymbol{H}} \boldsymbol{dx} \right) \right). \end{aligned} \tag{32}$$

Rewriting leads to

$$\begin{aligned} & r_x - \rho_2 \left(\left(\boldsymbol{Z}^{-1} \boldsymbol{r_z} - \boldsymbol{Z}^{-1} \boldsymbol{r_y} \boldsymbol{Y} \right) : \boldsymbol{I} \right) \boldsymbol{g}^{(2)} + \boldsymbol{\mathcal{X}}^T \cdot \left(\boldsymbol{Z}^{-1} \boldsymbol{r_z} - \boldsymbol{Z}^{-1} \boldsymbol{r_y} \boldsymbol{Y} \right) \\ & - \hat{\boldsymbol{G}}^T \cdot \boldsymbol{S_g}^{-1} \cdot \boldsymbol{r_{s_g}} + \hat{\boldsymbol{G}}^T \cdot \boldsymbol{S_g}^{-1} \cdot \boldsymbol{\lambda} \cdot \boldsymbol{r_\lambda} - \hat{\boldsymbol{H}}^T \cdot \boldsymbol{S_h}^{-1} \cdot \boldsymbol{r_{s_h}} + \hat{\boldsymbol{H}}^T \cdot \boldsymbol{S_h}^{-1} \cdot \boldsymbol{\gamma} \cdot \boldsymbol{r_\gamma} = \\ & \boldsymbol{H_i} \cdot \boldsymbol{dx} - \rho_2 \left(\left(\boldsymbol{Z}^{-1} \left(\boldsymbol{\mathcal{X}} \cdot \boldsymbol{dx} \right) \boldsymbol{Y} \right) : \boldsymbol{I} \right) \boldsymbol{g}^{(2)} + \rho_2^2 \left(\boldsymbol{Z}^{-1} \left(\boldsymbol{g}^{(2)T} \right) \boldsymbol{dx} \boldsymbol{I} \boldsymbol{Y} : \boldsymbol{I} \right) \boldsymbol{g}^{(2)} + \\ & \boldsymbol{\mathcal{X}}^T \boldsymbol{Z}^{-1} \left(\boldsymbol{\mathcal{X}} \cdot \boldsymbol{dx} \right) \boldsymbol{Y} - \rho_2 \boldsymbol{\mathcal{X}}^T \boldsymbol{Z}^{-1} \left(\boldsymbol{g}^{(2)T} \boldsymbol{dx} \right) \boldsymbol{I} \boldsymbol{Y} + \\ & \left(\hat{\boldsymbol{G}}^T \cdot \boldsymbol{S_g}^{-1} \cdot \boldsymbol{\lambda} \cdot \hat{\boldsymbol{G}} \right) \cdot \boldsymbol{dx} + \left(\hat{\boldsymbol{H}}^T \cdot \boldsymbol{S_h}^{-1} \cdot \boldsymbol{\gamma} \cdot \hat{\boldsymbol{H}} \right) \cdot \boldsymbol{dx}. \end{aligned} \tag{33}$$

The part related to the positive semi-definite constraint, line three and four in eq. (33), needs to be rewritten in the form $\boldsymbol{V} \cdot \boldsymbol{dx}$. Most parts can be written as (sum of) 2-dimensional arrays:

$$\begin{aligned} \boldsymbol{\mathcal{X}}^T \boldsymbol{Z}^{-1} \left(\boldsymbol{g}^{(2)T} \boldsymbol{dx} \right) \boldsymbol{I} \boldsymbol{Y} &= \boldsymbol{\mathcal{X}}^T \boldsymbol{Z}^{-1} \boldsymbol{Y} \cdot \boldsymbol{g}^{(2)T} \boldsymbol{dx} = \sum_i \boldsymbol{X_i}^T \boldsymbol{Z}^{-1} \boldsymbol{Y} \cdot \boldsymbol{g}^{(2)T} dx_i = \boldsymbol{b}^{(2)} \boldsymbol{g}^{(2)} \boldsymbol{dx} \\ \left(\boldsymbol{Z}^{-1} \left(\boldsymbol{\mathcal{X}} \cdot \boldsymbol{dx} \right) \boldsymbol{Y} : \boldsymbol{I} \right) \boldsymbol{g}^{(2)} &= tr \left(\boldsymbol{Z}^{-1} \left(\boldsymbol{\mathcal{X}} \cdot \boldsymbol{dx} \right) \boldsymbol{Y} \right) \boldsymbol{g}^{(2)} = \sum_i tr \left(\boldsymbol{Z}^{-1} \boldsymbol{X_i} \boldsymbol{Y} \right) \boldsymbol{g}^{(2)} dx_i = \boldsymbol{b}^{(1)} \boldsymbol{g}^{(2)} \boldsymbol{dx} \\ \left(\boldsymbol{Z}^{-1} \left(\boldsymbol{g}^{(2)T} \boldsymbol{dx} \right) \boldsymbol{I} \boldsymbol{Y} : \boldsymbol{I} \right) \boldsymbol{g}^{(2)} &= tr \left(\boldsymbol{Z}^{-1} \left(\boldsymbol{g}^{(2)T} \boldsymbol{dx} \right) \boldsymbol{I} \boldsymbol{Y} \right) \boldsymbol{g}^{(2)} = tr \left(\boldsymbol{Z}^{-1} \boldsymbol{Y} \right) \boldsymbol{g}^{(2)} \boldsymbol{g}^{(2)T} \boldsymbol{dx} = \boldsymbol{H^{(7)}} \boldsymbol{dx}, \end{aligned} \tag{34}$$

with

$$\begin{aligned} \boldsymbol{b} &= tr\left(\boldsymbol{Z}^{-1}\boldsymbol{X_i}\boldsymbol{Y}\right) \\ \boldsymbol{H^{(7)}} &= tr\left(\boldsymbol{Z}^{-1}\boldsymbol{Y}\right)\boldsymbol{g}^{(2)}\boldsymbol{g}^{(2)T}. \end{aligned} \tag{35}$$

For the first part of the fourth line this cannot be done. Hence, it is rewritten as

$$\boldsymbol{\mathcal{X}}^T\boldsymbol{Z}^{-1}\left(\boldsymbol{\mathcal{X}}\cdot\boldsymbol{dx}\right)\boldsymbol{Y} = \boldsymbol{\mathcal{X}}^T\boldsymbol{Z}^{-1}\boldsymbol{\mathcal{X}}^T\cdot\boldsymbol{Y}\cdot\boldsymbol{dx} = \boldsymbol{H^{(6)}}\cdot\boldsymbol{dx}. \tag{36}$$

Since the 3-dimensional arrays are not defined in a matrix-environment, one has to use

$$\boldsymbol{H^{(6)}}_{ij} = \left[\boldsymbol{\mathcal{X}}^T\boldsymbol{Z}^{-1}\boldsymbol{\mathcal{X}}^T\cdot\boldsymbol{Y}\right]_{ij} = \left(\boldsymbol{X_i}\cdot\boldsymbol{Z}^{-1}\cdot\boldsymbol{X_j}\right):\boldsymbol{Y}. \tag{37}$$

To determine the primal step size, the slack $\boldsymbol{Z}$ should stay positive semi-definite; to determine the dual step size, the dual variable $\boldsymbol{Y}$ should stay positive semi-definite. Using

$$\left(\boldsymbol{Z}+\eta\boldsymbol{dZ}\right)\boldsymbol{a} = \boldsymbol{0} \tag{38}$$

the maximum step size is the smallest negative eigenvalue.

Observing the equations in this appendix, it is noticed that only the expression for r_x and the Hessian are influenced by the additional constraints. Hence, posing multiple constraints in the same optimisation problem only influences these expressions, the size of the problem that is solved is not influenced.

References

[1] C. Kassapoglou, *Design and analysis of composite structures*. John Wiley and Sons, Ltd, 2010.

[2] "Boeing 787 from the gound up." `http://www.boeing.com/commercial/aeromagazine/articles/qtr_4_06/AERO_Q406_article4.pdf`. Accessed: 10 November 2015.

[3] "A350xwb technology." `http://www.airbus.com/aircraftfamilies/passengeraircraft/a350xwbfamily/technology-and-innovation`. Accessed: 10 November 2015.

[4] F.-X. Irisarri, A. Lasseigne, F.-H. Leroy, and R. L. Riche, "Optimal design of laminated composite structures with ply drops using stacking sequence tables," *Composite Structures*, vol. 107, no. 0, pp. 559 – 569, 2014.

[5] M. Bloomfield, J. Herencia, and P. Weaver, *Optimisation of Anisotropic Composite Plates Incorporating Non-Conventional Ply Orientations*. American Institute of Aeronautics and Astronautics, 2016/04/22 2008.

[6] M. Bruyneel, C. Beghin, G. Craveur, S. Grihon, and M. Sosonkina, "Stacking sequence optimization for constant stiffness laminates based on a continuous optimization approach," *Structural and Multidisciplinary Optimization*, vol. 46, no. 6, pp. 783–794, 2012.

[7] S. Zein, P. Basso, and S. Grihon, "A constraint satisfaction programming approach for computing manufacturable stacking sequences," *Computers & Structures*, vol. 136, pp. 56–63, 2014.

[8] H. Ghiasi, D. Pasini, and L. Lessard, "Optimum stacking sequence design of composite materials part i: Constant stiffness design," *Composite Structures*, vol. 90, no. 1, pp. 1 – 11, 2009.

[9] S. Honda, Y. Narita, and K. Sasaki, "Discrete optimization for vibration design of composite plates by using lamination parameters," *Advanced Composite Materials*, vol. 18, no. 4, pp. 297–314, 2009.

[10] S. Liu, Y. Hou, X. Sun, and Y. Zhang, "A two-step optimization scheme for maximum stiffness design of laminated plates based on lamination parameters," *Composite Structures*, vol. 94, no. 12, pp. 3529 – 3537, 2012.

[11] G. Raju, S. White, Z. Wu, and P. Weaver, *Optimal Postbuckling Design of Variable Angle Tow Composites using Lamination Parameters*. American Institute of Aeronautics and Astronautics, 2015/03/30 2015.

[12] R. LE RICHE and R. T. HAFTKA, "Optimization of laminate stacking sequence for buckling load maximization by genetic algorithm," *AIAA Journal*, vol. 31, pp. 951–956, 2015/05/18 1993.

[13] F. Aymerich and M. Serra, "Optimization of laminate stacking sequence for maximum buckling load using the ant colony optimization (aco) metaheuristic," *Composites Part A: Applied Science and Manufacturing*, vol. 39, no. 2, pp. 262 – 272, 2008.

[14] Z. Gürdal, B. Tatting, and K. Wu, "Tow-placement technology and fabrication issues for laminated composite structures," in *46th AIAA/ASME/ASCE/AHS/ASC Structures, Structural Dynamics and Materials Conference*, American Institute of Aeronautics and Astronautics, 2014/11/30 2005.

[15] M. Hyer and H. Lee, "The use of curvilinear fiber format to improve buckling resistance of composite plates with central circular holes," *Composite Structures*, vol. 18, no. 3, pp. 239 – 261, 1991.

[16] Z. Gürdal and R. Olmedo, "In-plane response of laminates with spatially varying fiber orientations - variable stiffness concept," *AIAA Journal*, vol. 31, pp. 751–758, 2014/11/30 1993.

[17] D. M. Peeters, S. Hesse, and M. M. Abdalla, "Stacking sequence optimisation of variable stiffness laminates with manufacturing constraints," *Composite Structures*, vol. 125, no. 0, pp. 596 – 604, 2015.

[18] C. Fleury, "Conlin: An efficient dual optimizer based on convex approximation concepts," *Structural optimization*, vol. 1, no. 2, pp. 81–89, 1989.

[19] K. Svanberg, "a class of globally convergent optimization methods based on conservative convex separable approximations," *Siam J. optim*, vol. 2, pp. 555–573, 2002.

[20] G. Vanderplaats and H. Thomas, "An improved approximation for stress constraints in plate structures," *Structural optimization*, vol. 6, no. 1, pp. 1–6, 1993.

[21] S. W. Tsai and H. Hahn, *Introduction to composite materials*. Technomic, Westport, 1989.

[22] V. Hammer, M. Bendsøe, R. Lipton, and P. Pedersen, "Parametrization in laminate design for optimal compliance," *International Journal of Solids and Structures*, vol. 34, no. 4, pp. 415 – 434, 1997.

[23] S. Setoodeh, M. M. Abdalla, S. T. IJsselmuiden, and Z. Gürdal, "Design of variable-stiffness composite panels for maximum buckling load," *Composite Structures*, vol. 87, no. 1, pp. 109 – 117, 2009.

[24] S. T. Ijsselmuiden, M. M. Abdalla, and Z. Gürdal, "Optimization of variable-stiffness panels for maximum buckling load using lamination parameters," *AIAA Journal*, vol. 48, no. 1, pp. 134–143, 2010.

[25] A. Khani, S. IJsselmuiden, M. Abdalla, and Z. Grdal, "Design of variable stiffness panels for maximum strength using lamination parameters," *Composites Part B: Engineering*, vol. 42, no. 3, pp. 546 – 552, 2011.

[26] A. Blom, S. Setoodeh, J. Hol, and Z. Gürdal, "Design of variable-stiffness conical shells for maximum fundamental eigenfrequency," *Computers and Structures*, vol. 86, no. 9, pp. 870 – 878, 2008.

[27] M. Abdalla, S. Setoodeh, and Z. Gürdal, "Design of variable stiffness composite panels for maximum fundamental frequency using lamination parameters," *Composite Structures*, vol. 81, no. 2, pp. 283 – 291, 2007.

[28] G. Thuwis, R. Breuker, M. Abdalla, and Z. Gürdal, "Aeroelastic tailoring using lamination parameters," *Structural and Multidisciplinary Optimization*, vol. 41, no. 4, pp. 637–646, 2009.

[29] J. K. S. Dillinger, T. Klimmek, M. M. Abdalla, and Z. Gürdal, "Stiffness optimization of composite wings with aeroelastic constraints," *Journal of Aircraft*, vol. 50, pp. 1159–1168, 2016/09/26 2013.

[30] M. M. Abdalla, C. Kassapoglou, and Z. Gürdal, "Formulation of composite laminate robustness constraint in lamination parameters space," in *50th AIAA/ASME/ASCE/AHS/ASC Structures, Structural Dynamics and Materials Conference*, American Institute of Aeronautics and Astronautics, 2009.

[31] C. Lopes, O. Seresta, M. Abdalla, Z. Gurdal, B. Thuis, and P. Camanho, *Stacking Sequence Dispersion and Tow-Placement for Improved Damage Tolerance*. American Institute of Aeronautics and Astronautics, 2015/05/26 2008.

[32] C. Lopes, P. Camanho, Z. Gürdal, P. Maim, and E. Gonzàlez, "Low-velocity impact damage on dispersed stacking sequence laminates. part ii: Numerical simulations," *Composites Science and Technology*, vol. 69, no. 78, pp. 937 – 947, 2009.

[33] M. Nagelsmit, C. Kassapoglou, and Z. Gürdal, "Ap-ply: A new fibre placement architecture for fabric replacement," *SAMPE Journal*, vol. 47, no. 2, pp. 36 – 45, 2011.

[34] L. Grunenfelder, N. Suksangpanya, C. Salinas, G. Milliron, N. Yaraghi, S. Herrera, K. Evans-Lutterodt, S. Nutt, P. Zavattieri, and D. Kisailus, "Bio-inspired impact-resistant composites," *Acta Biomaterialia*, vol. 10, no. 9, pp. 3997 – 4008, 2014. Biomineralization.

[35] T. Sebaey, E. Gonzlez, C. Lopes, N. Blanco, and J. Costa, "Damage resistance and damage tolerance of dispersed {CFRP} laminates: Design and optimization," *Composite Structures*, vol. 95, no. 0, pp. 569 – 576, 2013.

[36] S. W. Beckwith, "Designing with composites: Suggested best practices rules," *SAMPE journal*, vol. 45, pp. 36 – 37, 2009.

[37] J. Bailie, R. Ley, and A. Pasricha, "A summary and review of composite laminate design guidelines," *Langley RC, Hampton*, 1997.

[38] C. T. Herakovich, "On the relationship between engineering properties and delamination of composite materials," *Journal of Composite Materials*, vol. 15, pp. 336–348, 1981.

[39] S. T. IJsselmuiden, M. M. Abdalla, O. Seresta, and Z. Gürdal, "Multi-step blended stacking sequence design of panel assemblies with buckling constraints," *Composites Part B: Engineering*, vol. 40, no. 4, pp. 329 – 336, 2009.

[40] S. T. Ijsselmuiden, M. M. Abdalla, and Z. Gürdal, "Implementation of strength-based failure criteria in the lamination parameter design space," *AIAA Journal*, vol. 46, pp. 1826–1834, 2015/04/15 2008.

[41] S. W. Tsai and J. D. D. Melo, "An invariant-based theory of composites," *Composites Science and Technology*, vol. 100, no. 0, pp. 237 – 243, 2014.

[42] C. Zillober, "A combined convex approximationinterior point approach for large scale nonlinear programming," *Optimization and Engineering*, vol. 2, no. 1, pp. 51–73, 2001.